AADE-07-NTCE-67

Time-Dependent Wellbore Strengthening in Chemically Active or Less Active Rock Formations

Younane N. Abousleiman, Vinh Nguyen,The PoroMechanics Institute, The University of Oklahoma; Terry Hemphill, Halliburton; and Mazen Y. Kanj, EXPEC Advanced Research Center, Saudi Aramco

Abstract

Over the last two years, permeability has drawn much greater interest in the wellbore strengthening phenomenon. This interest culminated into proving that "Stress Cage" is a natural time-dependent process; occurring as a result of mud system additives, such as lost circulation materials (LCM), lost prevention materials (LPM) and other mud solid additives. In this study, we demonstrate through field applications and physical analyses that permeability engineering values and chemical enhancements to the mud system are of critical importance in wellbore fracture gradient increase and wellbore strengthening.

The modified poroelastic wellbore stability solution takes into account the time-lapse of mud circulation, mud and shale formation chemical potential, and the associated permeability mechanical effects. These mechanisms, when coupled in the general wellbore solution, exhibit a very intricate interplay on wellbore "strengthening" and its degradation and/or build-up with time. In addition, the solution demonstrates the interaction among (1) mud fines content and formation permeability with relation to the increase of wellbore fracture gradient, (2) the mud chemistry effects on that issue, and (3) the rock formation and wellbore wall in view of pressure communication and pressure transmission between the drilling mud and the formation pore fluids. Also, these applications illustrate the benefits of idle mud time-lapse circulation and the resulting effects on wellbore strengthening. For the first time, time-dependent effects are addressed in a wellbore fracturing solution that takes into consideration the chemical osmotic nature of water-base and oil-base muds while drilling. Finally, these solutions are implemented in a friendly interface environment, PBORE-3D© that makes it easier for a drilling engineer to operate and interpret real-time wellbore stability rig data.

Introduction

Wellbore strengthening in mature sandstone reservoirs and/or newly discovered sandstone reservoirs with shale formation stringers has drawn great interest lately in industry applications and in theoretical and physical modeling. These operations, when unsuccessful, have transpired into costly downtimes, magnified by frequent stuck-pipe issues and associated with extensive use of "grease pills" and/or drilling mud additives.

Wellbore strengthening techniques with Lost Circulation Materials (LCM), Lost Prevention Materials (LPM) and other mud additives have proven field successes in drilling operations worldwide.[1,2,3] However, some studies[4] used scenarios of fracture creation at the wellbore wall and applied particulate matter to the drilling fluid to attempt to bridge the fractures (if and when this ever took place), to reduce downhole mud losses. While the authors claimed an increase in the wellbore fracture gradient, through multiple fracture creation and bridging, they struggled mechanistically to explain exactly what was going on from a fracture mechanics point of view. They called it the "Stress Cage" phenomenon.

Literature-based field applications and theoretical explanations and modeling converge on one universal field observation that these "Stress Caging" techniques do not apply to low-permeability formations! [1] Yet, none of these existing studies included permeability, and in particular Darcy's law and Fick's law in their respective physical models to attempt to interpret the pressure diffusion and solute transport in wellbore strengthening phenomena.[5,6] Thus, a time-dependent pressure diffusion type equation coupled with stress analysis is a necessity. This type of analysis is somehow more mathematically involved, yet from the physics point of view, is very simple.[7,8,9,10] That is when rock mechanics is coupled with fluid flow, the permeability coefficient becomes an integral part of the solution to these problems. In this regard, the permeability and chemical osmotic effects go hand-in-hand when modeling shale rocks (very low permeability) and/or clayey formations exhibiting some form of chemical sensitivity to mud systems.

Much earlier studies on lost circulation while drilling have included non-linear mechanistic approaches to fracture initiation and propagation, in an attempt to explain mud losses.[11,12] Others[13], discussed approaches that has to do with wellbore inclination, and fracture creation and link ups using some nonlinear factors approximated from nonlinear numerical schemes. However, none of these studies addressed permeability variation at the wellbore wall, which occurs before or after any “fracture” creation, let alone propagation or even link ups, or any considerable amount of mud loss circulation.

On another front, LCMs and LPMs contain a distribution range of fine particles, i.e., coarse barite to fine barite, graphite, solid additives, etc. Over the correct range in particulate size(s), the mud system can plug the rock pores at the wellbore wall while circulating.[2,3] At a constant wellbore mud pressure, the borehole wall permeability becomes only a function of time. This is only possible in rock formations with medium to high permeability, and in particular, depleted sandstones.

Rock Mechanics and the Paramount Effects of Permeability: LPM/LCM and Wellbore Strengthening

The wellbore fracturing pressure or breakdown pressure is the limit to which the mud density can be increased in the well without fracturing the formation and possibly causing loss circulation. Conventionally, wellbore fracturing is assumed to occur when the effective tensile tangential stress at the wellbore wall exceeds the tensile strength of the formation. Conservatively, the tensile strength is assumed to be zero in most rocks for drilling planning and analysis. A tensile fracture would initiate if the breakdown pressure (or mud density) is higher or equal to the compressive tangential stresses (neglecting tensile rock strength). This fracture would be prone to propagate and cause loss of circulation, if and only if, it reaches a critical length where the regional stresses (far field in-situ stresses) come into play and in particular the minimum principle in-situ stress. How could the wellbore fracture gradient be much larger than the minimum horizontal stress (S_h) and if so, when? The whole approach in rock mechanics to wellbore stability has focused in the past on wellbore collapse, only few studies have addressed the time-dependent pressure term to wellbore fracturing and fracture gradient estimation.

General Practices

Fracture gradient in the conventional rock mechanics analysis is expressed by the well known Kirsch solution for tangential stress assuming vertical wellbore (compression is considered positive)

$$\sigma'_{\theta\theta-\min} = \sigma_{\theta\theta-\min} - p = (3S_h - S_H - p_w) - p_w \qquad (1)$$

$$\sigma'_{\theta\theta-\min} = \sigma_{\theta\theta-\min} - p = (3S_h - S_H - p_w) - p_f \qquad (2)$$

where $\sigma'_{\theta\theta-\min}$ is the minimum effective tangential stress at the borehole wall (along the maximum horizontal stress), $\sigma_{\theta\theta-\min}$ is the total tangential stress, S_h and S_H are the minimum and maximum horizontal in-situ stresses, p is the fluid pressure in the porous rock taken as either the wellbore mud pressure p_w or the formation virgin pore pressure p_f.

So, what controls the use of Eq. (1) and Eq. (2)? Eq. (1) has been almost universally used as the upper limit of wellbore frac-gradient, WFG. This is only true, if perfect wellbore/formation fluid pressure communication exist and is instantaneous. That is time pressure diffusion from wellbore wall into the formation is instant. Critical fracturing mud pressure under this condition is given by

$$p_c = (3S_h - S_H)/2 = \left(1.5 * S_h / S_H - 0.5\right)S_H \qquad (3)$$

Setting $p_c > S_h$ in Eq. (3) leads to the impossible condition $S_h > S_H$. Therefore, the critical fracturing mudweight is always less than the minimum horizontal stress, S_h, for the fully-permeable boundary condition at the borehole wall. Thereafter, this critical breakdown pressure is termed the Kirsch fracturing gradient lower limit (KFGLL).

On the other hand, Eq. (2) assumes a non-penetrating fluid condition, i.e., no pressure communication between the wellbore and the formation. The critical fracturing pressure becomes

$$p_c = 3S_h - S_H - p_f = (3S_h / S_H - p_f / S_H - 1)S_H \qquad (4)$$

Fig. 1 plots the regions of in-situ condition for different bounds of critical fracturing mudweight values for the impermeable wellbore wall condition. The x-axis represents the ratio of pore pressure and maximum horizontal stress, i.e. $x \equiv p_f/S_H$; the y axis is the ratio of minimum and maximum horizontal stress, i.e. $y \equiv S_h/S_H$. According to Eq. (4), the wellbore will always undergo tensile fracturing for any mudweight condition ($p_c < 0$) when the ratios of S_h/S_H and p_f/S_H fall into the region below the line $y = (1+x)/3$. The region between the line $y = (1+x)/3$ and $y = (1+x)/2$ yields a breakdown pressure less than the minimum horizontal stress, $p_c < S_h$. The next region bounded by the lines $y = (1+x)/2$ and $y = (2+x)/3$ gives a fracturing mudweight larger than S_h but less than S_H. The top region above the line $y = (2+x)/3$ predicts critical fracturing mudweights that are even larger than the maximum horizontal stress S_H, for example, $p_c = 1.5*S_H$ when $S_h = S_H$ and $p_f = 0.5* S_H$. Hence, under these conditions this fracturing mudweight can be termed the Kirsch fracturing gradient upper limit (KFGUL). The top two regions are possible candidates for wellbore strengthening concept such as “Stress Cage”.

Alberty and Mclean [4] field data when analyzed under the aforementioned approaches fall significantly below the KFGUL. The obvious field condition in their work is the in-situ horizontal stresses are almost of equal magnitude as shown in Fig. 1. Table 1 compares the critical fracturing mudweight results calculated using the Kirsch permeable and impermeable wall models described above and the “Stress Cage” model for the two sets of in-situ condition (A and B)[4] in depleted sandstone formations. The “Stress Cage” model predicts that after applying bridging material, the total stress state near the bridge has risen and thus higher fracture gradient is attained. However, the Kirsch solution shows that by changing our assumptions in the wellbore/formation wall conditions two limiting fracture gradients (effective tangential stress) can be attained whereas the total stress state remains unaltered as illustrated in Fig. 2 to 4. This shows why most of the strengthening techniques such as LCM, LPM and/or "Stress Cage" do not work in "low permeability formations."[1,4] In addition, the results clearly show that although the "Stress Cage" suggested drilling mudweights with bridging material (14.4 ppg) are higher than the maximum in-situ stress (12.6 ppg) these mudweights are well below the fracture gradient as predicted by the Kirsch solution for "impermeable wall condition" (17.2 ppg). In Fig. 1, the two cases examined herein (A and B) fall right into the region having WFG higher than the maximum in-situ stress.

Permeability and Fracture Gradient

Physically it is impossible, in a fluid saturated porous "rock" when subjected to stress and fluid pressure, to assume that fluid/pressure diffusion from the wellbore into the formation is either instantaneous or non-existing ("fully-permeable" or "fully impermeable" conditions). In fact, it is a transient, time-dependent, and time-controlled process.

This phenomenon is very well known and documented since Fourier's Law[14] to Darcy's law.[15,16] In our case for wellbore pressure diffusion process based on Biot's theory of poroelasticity,[7] the controlling factors are permeability magnitude, pressure gradient, and the applied stresses. In other words, taking the pore pressure p as a constant equals to either p_f or p_w is only conceptual. As such, the pore pressure is a function of time, $p = p(t)$. Moreover, the transient fluid flow through the porous rock formations gives rise to coupled time-dependent stress responses, $\sigma_{\theta\theta} = \sigma_{\theta\theta}(t)$. As a result, the time-independent Kirsch solution is no more applicable. The correct rock mechanics/poroelastic approach to determine fracture gradient, with the effective stress concept, or Terzaghi's principle, must be modified as

$$\sigma'_{\theta\theta-\min}(t) = \sigma_{\theta\theta-\min}(t) - \alpha\, p(t) \quad (5)$$

Where α is the Biot Pore Pressure Coefficient, PPC = (1-C_s/C) in which, C is the porous rock matrix compressibility, and C_s is rock grain compressibility.[7,26] In the special case of α = 1, the above Biot effective stress is reduced to the wellknown Terzaghi effective stress. The mechanics and models explaining in details these phenomena are very well documented in hydraulic fracture initiation and propagation,[17] subsidence and in reservoir stimulation.[10,18] The initial poroelastic solutions to Eq. (5) for plane strain condition, e.g., vertical wellbore was published by Haimson and Fairhurst.[17] The time-dependent part of the solution assumed equal in-situ stresses, leading to constant fracture gradient at the wellbore wall, that is permeability-independency occurs only under such a condition. Recently, the general solution to the inclined wellbore geometry in a three dimensional state of stress has been published.[19,20] These solutions take into account the full poroelastic coupling of fluid flow/solid deformation in which engineering values for permeability are fully integrated into the wellbore fracture gradient solution, leading to time-dependent estimation of fracture gradient at the borehole wall, and physically illustrating the effects of the coefficient of permeability variations. For complementing the analysis, the poroelastic solution for $\sigma_{\theta\theta-\min}(t)$ and $p(t)$ are presented in the Appendix of this paper, including the special cases for vertical wellbore and/or hydrostatic state of stresses.[17]

Fig. 5 shows typical time variations of pore pressure *p(t)* in the formation along the maximum in-situ stress direction. The pore pressure is not simply varying monotonously from the wellbore pressure p_w to the formation pressure p_f at far field. The near wellbore pressure dip below p_f is due to the poroelastic effect caused by unequal in-situ horizontal stress field, which prevails in most field applications.

Fig. 6 shows a schematic of permeability reduction with time due to mud circulation and plugging effect of LCM/LPM materials. Fig. 7 to 11 plots the effective tangential stress, e.g., fracture gradients, at and around the wellbore wall at critical fracturing mudweights for the elastic model with permeable and impermeable wall conditions and poroelastic model at three values of permeability. In addition, the poroelastic results show four time intervals through the drilling operation. This analysis is conducted using a general purpose wellbore stability simulator PBORE-3D©[21,22,23] developed by the PoroMechanics Institute at the University of Oklahoma. Fig. 7 and 8 show the Kirsh lower and upper limit for critical fracturing mudweight by employing the elastic permeable and impermeable models in PBORE-3D©. Fig. 9 to 11 show the effect of varying the values of the permeability on fracture gradient calculation. All the mudweight results are tabulated in Table 2 from which the following observations can be made

i. Kirsh elastic solution with the conceptual approaches of permeable and impermeable borehole wall conditions provides too simple of an estimation of the bounds for fracture gradient.
ii. The integration of permeability coefficient in the poroelastic solution gives much less conservative fracture gradient prediction than the elastic permeable counterpart.
iii. The higher permeability values show that the formations sustain less breakdown pressure. In other words, decreasing the near wellbore permeability helps strengthen the fracture gradient, in our simulated case, as much as 1.32 ppg.
iv. Finally, it is clear that the wellbore fracture gradient is not a constant; rather it evolves with the time of drilling. For example, the predicted fracture gradient drops approximately 1.32 ppg (from 17.72 ppg to 16.40 ppg) after 1 day of exposed drilling fluid to the formation with permeability of 10^{-2} mD. On the other hand, the drop is only 0.72 ppg (from 18.01 ppg to 17.28 ppg) after 1 day of exposed drilling fluid to the formation with permeability of 10^{-5} mD. Hence, the

poroelastic solution provides a useful tool for the prediction of the time window from fracture gradient to wellbore collapse for drilling planning and operation.

Chemical Strengthening Effect

In chemically active shale formation, the driving total pressure P, for the total fluid flow comprises of the pore pressure p and the osmotic pressure $p_{osmotic}$ accounting for the chemical activity such that

$$\mathrm{P} = p + p_{osmotic} \tag{6}$$

with the osmotic pressure given by the well-known relation

$$p_{osmotic} = \chi \frac{RT}{V_f} \ln(a^f) \tag{7}$$

where V_f is the molar volume of water, χ is the reflection coefficient or membrane efficiency which varies between 0 for chemically inert media and 1 for perfect ion exclusion materials, R is the universal gas constant, T is the absolute temperature and a^f is the dimensionless mud/shale water activities which is a function of salinity and temperature. From Eq. (7), osmotic pressures are due to a gradient in the pore fluid chemical activity or equivalently salinity. As a result, the Darcy bulk fluid flow in chemically active formation is controlled not only by the permeability magnitude, pore pressure but also osmotic pressure gradient. For example, a drilling mud with higher activity (lower salinity) than the formation fluid will induce an osmotic flow into the formation and increase the pore pressure in side the formation. This further intensifies wellbore instability conditions, especially in term of the fracture gradient. However, a drilling mud with lower activity (higher salinity) will induce an osmotic backflow from the formation into the wellbore, thereby reducing the near wellbore pressure and providing stabilizing support to the wellbore.

On the other hand, there is also transport/diffusion flux of solute species (salt, ions, etc.) existing in the pore fluid due to solute salinity/activity gradient between the wellbore fluid and the formation fluid that follow Fick's first law of diffusion.[24] The Fick's solute diffusion occurs simultaneously with the bulk Darcy flow during drilling operations and will gradually equilibrate the salinity/activity gradient between the wellbore and the formation. Consequently, the osmotic effect is also a time-dependent process, $p_{osmotic} = p_{osmotic}(t)$. Moreover under the framework of the theory of poroelasticity, these Darcy's and Fick's flows must be coupled with the applied stress fields for proper modeling. The general porochemoelastic inclined wellbore solution incorporating solute transport is more mathematically involved and has been published[25] and will not be presented in this work. A simplified solution approach using the total pressure P, however, is presented in the Appendix.

Fig. 12 shows the minimum effective stress after 2.4 hours into drilling. For comparison purpose, the elastic solution is also plotted. For non reactive formation such as sandstone (reflection coefficient χ = 0), the solution reduces to the normal poroelastic solution without chemical effect. In highly-reactive formations, high mud salinity reduces the near wellbore pressure and provides strengthening effect to the fracture gradient. Conversely, in these same formations, low mud salinity condition enhances the near wellbore pressure and weakens the fracture gradient.

Fig. 13 shows the fracture gradient strengthening effect with time. This implies that the interaction among the drilling fluid fine content, chemical activity, formation mechanical deformation and fluid transmission (permeability) can be played under specific condition to achieve reasonable strengthening effect.

Conclusions

In this work, a consistent engineering approach to modeling wellbore fracture gradient integrating the important effect of permeability and chemical osmotic has been successfully performed, leading to time-dependent mud window for well planning/operations.

Analyses show that the conventional Kirsch elastic solution with the conceptual approaches of permeable and impermeable conditions provides too simple of an estimation of the bounds for fracture gradient.

Permeability has a profound effect on the wellbore fracture gradient. The integration of permeability coefficient in the poroelastic solution gives much less conservative fracture gradient prediction than the elastic permeable counterpart. It is also found that decreasing the near wellbore permeability increases substantially the fracture gradient, thus "wellbore strengthening". However, the strengthening effect is a time-lapsed process. Therefore, the general poroelastic solution provides the necessary tool for the prediction of the time window for fracture gradient strengthening effect.

Finally, it has also been shown that the permeability and chemical osmotic effects can be altered under specific field conditions to achieve desirable strengthening effect.

Acknowledgments

The third author thanks Halliburton for the permission to publish this paper. Partial funds for this work were provided by the PoroMechanics Institute, through the Rock Mechanics Consortium members.

Appendix

In their initial solution for vertical wellbore, Haimson and Fairhurst expressed the effective tangential stress as (compression is positive)

$$\begin{aligned}\sigma_{\theta\theta}(t) = {} & 0.5(S_H + S_h)(1 + \frac{R^2}{r^2}) \\ & - 0.5(S_H - S_h)(1 + 3\frac{R^4}{r^4})\cos(2\theta) \\ & - p_w \frac{R^2}{r^2} + 2\eta(p_w - p_f) * \sigma_{\theta\theta}^{(1)}(t)\end{aligned} \tag{A1}$$

$$p(t) = p_f + (p_w - p_f) p^{(1)}(t) \qquad \text{(A2)}$$

where R is the wellbore radius, θ is the angle around the wellbore, and η is the poroelastic coefficients defined as

$$\eta = \frac{\alpha(1-2\nu)}{2(1-\nu)} \qquad \text{(A3)}$$

where α is the pore pressure coefficient – PPC, [26] ν is the Poisson ratio, and $\sigma_{\theta\theta}^{(1)}(t)$ and $p^{(1)}(t)$ are the time-dependent part of the stress and pore pressure due to fluid /pressure diffusion in the formation

$$\sigma_{\theta\theta}^{(1)}(t) = L^{-1}\left\{ \frac{1}{sr\xi}\frac{K_1(r\xi)}{K_0(R\xi)} - \frac{R}{sr^2\xi}\frac{K_1(R\xi)}{K_0(R\xi)} + \frac{1}{s}\frac{K_0(r\xi)}{K_0(R\xi)} \right\} \text{(A4)}$$

$$p^{(1)}(t) = L^{-1}\left\{ \frac{1}{s}\frac{K_0(r\xi)}{K_0(R\xi)} \right\} \qquad \text{(A5)}$$

in which s is the Laplace variable, K_0, and K_1 are modified Bessel functions. The effect of permeability k is manifested in the term $\xi = \sqrt{s/c}$ where c is the lumped poroelastic diffusivity given as

$$c = \frac{k}{\mu}\frac{2G(1-\nu)(\nu_u - \nu)}{\alpha^2(1-\nu_u)(1-2\nu)^2} \qquad \text{(A6)}$$

where μ is the dynamic fluid viscosity, G is the shear modulus, ν_u is the undrained Poisson's ratio.

At the borehole wall $r = R$, Eq. (A4) and (A5) reduce to a constant value of 1. Thus, the minimum effective tangential stress which occurs along the maximum horizontal stress direction, i.e., $\theta = 0^o$, 180^o, is a constant

$$\begin{aligned}\sigma'_{\theta\theta-\min}(R) &= \sigma_{\theta\theta-\min}(R) - p_w \\ &= 3S_h - S_H - 2p_w + 2\eta(p_w - p_f)\end{aligned} \qquad \text{(A7)}$$

As a result, the critical fracturing mudweight is also a constant and obviously time-independent

$$p_c = \frac{3S_h - S_H - 2\eta p_f}{2(1-\eta)} \qquad \text{(A8)}$$

The above solution is limited to vertical wellbore geometry and ignores the solid rock deformation coupling onto the fluid flow. The complete poroelastic solution for the stress/pore pressure distribution around wellbore drilled in porous saturated rock formations have been derived.[19] For general inclined wellbore geometry, the pore pressure and total tangential stress are expressed as

$$\begin{aligned}\sigma_{\theta\theta}(t) &= 0.5(S_x + S_y)(1 + \frac{R^2}{r^2}) \\ &\quad - p_w\frac{R^2}{r^2} + 2\eta(p_w - p_f) * \sigma_{\theta\theta}^{(1)}(t) \\ &\quad - 0.5(S_x - S_y)[1 + \sigma_{\theta\theta}^{(2)}(t)]\cos(2\theta)\end{aligned} \qquad \text{(A9)}$$

$$\begin{aligned}p(t) &= p_f + (p_w - p_f) p^{(1)}(t) \\ &\quad + 0.5(S_x - S_y) * p^{(2)}(t)\cos(2\theta)\end{aligned} \qquad \text{(A10)}$$

where S_x and S_y are the stresses obtained by rotating the in-situ three dimensional state of stress $\{S_H, S_h, S_V\}$ into the incline wellbore coordinate, $p^{(2)}(t)$ and $\sigma_{\theta\theta}^{(2)}(t)$ are expressed as inversed Laplace transforms (L^{-1}) of

$$p^{(2)}(t) = L^{-1}\left\{ \begin{aligned} &\frac{B^2(1-\nu)(1+\nu_u)^2}{9s(1-\nu_u)(\nu_u - \nu)} C_1 K_2(r\xi) \\ &+ \frac{B(1+\nu_u)}{3s(1-\nu_u)} C_2 \frac{R^2}{r^2} \end{aligned} \right\} \qquad \text{(A11)}$$

$$\sigma_{\theta\theta}^{(2)}(t) = L^{-1}\left\{ \begin{aligned} &-\frac{B(1+\nu_u)}{3s(1-\nu_u)} C_1 \left(\frac{K_1(r\xi)}{r\xi} + (1 + \frac{6}{(r\xi)^2}) K_2(r\xi) \right) \\ &+ \frac{3C_3}{s}\frac{R^4}{r^4} \end{aligned} \right\} \qquad \text{(A12)}$$

where B is Skepmton coefficient, C_1, C_2 and C_3 are lumped parameters defined as

$$C_1 = -\frac{12R\xi(1-\nu_u)(\nu_u - \nu)}{B(1+\nu_u)(D_2 - D_1)} \qquad \text{(A13)}$$

$$C_2 = \frac{2(1-\nu_u)D_2}{D_2 - D_1} \qquad \text{(A14)}$$

$$C_3 = -\frac{R\xi(D_2 - D_1) + 8(\nu_u - \nu)K_2(R\xi)}{R\xi(D_2 - D_1)} \qquad \text{(A15)}$$

the constants D_1 and D_2 are given by

$$D_1 = 2(\nu_u - \nu)K_1(R\xi) \qquad \text{(A16)}$$

$$D_2 = R\xi(1-\nu)K_2(R\xi) \qquad \text{(A17)}$$

For the special case of vertical wellbore, $S_x \equiv S_H$ and $S_y \equiv S_h$, the minimum effective tangential stress at the borehole wall $r = R$ reduces to

$$\sigma'_{\theta\theta-\min}(R,t) = \sigma_{\theta\theta-\min}(R,t) - p_w$$
$$= 0.5(S_H + 3S_h) - 2p_w + 2\eta(p_w - p_f) \quad \text{(A18)}$$
$$-0.5(S_H - S_h)\sigma^{(2)}_{\theta\theta}(R,t)$$

Eq. (A18) shows that at the borehole wall, the effective tangential stress is varying with time due to the coupled fluid diffusion/solid deformation effect and the rate of variation is clearly permeability-dependent. The fracture gradient for this case is

$$p_c = \frac{0.5(S_H + 3S_h) - 0.5(S_H - S_h)\sigma^{(2)}_{\theta\theta}(R,t) - 2\eta p_f}{2(1-\eta)} \quad \text{(A19)}$$

In addition, if the horizontal stresses are of equal magnitudes S_h = S_H, then both Eq. (A8) of Haimson and Fairhurst and Eq. (A19) reduces to

$$p_c = \frac{S_H - \eta p_f}{1-\eta} \quad \text{(A20)}$$

For chemical active formation, the solution is more involved. A first order approach is to replace the pore pressure in the poroelastic solution by the total pressure P = $p + p_{osmotic}$ in Eq. (6) that includes the osmotic pressure effect. As such, the tangential stress and pore pressure for a chemically active rock formation can be expressed as

$$\sigma_{\theta\theta}(t) = 0.5(S_H + S_h)(1 + \frac{R^2}{r^2})$$
$$- p_w \frac{R^2}{r^2} + 2\eta(p_w + p_{osmotic} - p_f) * \sigma^{(1)}_{\theta\theta}(t) \quad \text{(A21)}$$
$$-0.5(S_H - S_h)[1 + \sigma^{(2)}_{\theta\theta}(t)]\cos(2\theta)$$

$$p(t) = p_f + (p_w + p_{osmotic} - p_f)p^{(1)}(t)$$
$$+ 0.5(S_H - S_h) * p^{(2)}(t)\cos(2\theta) \quad \text{(A22)}$$

From Eq. (A21) and (A22), it can be seen that the permeability and osmotic effect are necessary parameters when modeling chemically active rock formations.

Nomenclature

a^f	= *Mud/formation activity ratio*
B	= *Skempton coefficient*
c	= *Lumped poroelastic diffusivity*
G	= *Shear modulus*
k	= *Formation permeability*
KFGLL	= *Kirsh fracture gradient lower limit*
KFGUL	= *Kirsh fracture gradient upper limit*
LCM	= *Lost circulation materials*
LPM	= *Lost prevention materials*
MHS	= *Minimum horizontal stress*
p	= *pore pressure*
p_f	= *formation virgin pore pressure (far field)*
$p_{osmotic}$	= *osmotic pressure*
p_w	= *wellbore mud pressure*
P	= *total pressure (=* $p + p_{osmotic}$*)*
S_h	= *Minimum horizontal stress*
S_H	= *Maximum horizontal stress*
r	= *radial distance into the formation*
R	= *Wellbore radius*
t	= *time*
T	= *Formation temperature*
V_f	= *Water molar volume*
WFG	= *Wellbore fracture gradient*

Greek Symbols

α	= *Pore pressure coefficient*
η	= *Poroelastic constant*
μ	=*Fluid viscosity*
ν	= *Poisson ratio*
ν_u	= *Undrained Poisson ratio*
θ	= *Angle around the wellbore*
χ	= *Reflection coefficient*
$\sigma_{\theta\theta}$	= *Total tangential stress*
$\sigma_{\theta\theta-min}$	= *Minimum tangential stress*
$\sigma'_{\theta\theta}$	= *Effective tangential stress*

References

1. Dupriest, F. E.: "Fracture Closure Stress (FCS) and Lost Returns Practices," Paper SPE 92192, presented at the 2005 SPE/IADC Drilling Conference held in Amsterdam, The Netherland, February 23-25.
2. Davison, J. M., Leaper, R., Cauley, M. B., Bennett, B., Mackenzie, A., Higgins, C. J., Shuttleworth, N., and Wilkinson, D.: "Extending the Drilling Operating Window in Brent: Solutions for Drilling in Depleting Reservoirs," Paper SPE 87174, presented at the 2004 IADC/SPE Drilling Conference held in Dallas, Texas, USA, March 2-4.
3. Benaissa, S., Bachelot, A., and Ong, S.: "Preventing Mud Losses and Differential Sticking by Altering Effective Stress of Depleted Sands," Paper SPE 103816, presented at the 2006 IADC/SPE Asian Pacific Drilling Conference and Exhibition held in Bangkok, Thailand, 13-15 November.
4. Alberty, M. W. and McLean, M.R.: "A Physical Model for Stress Cages," Paper SPE 90493, presented at the 2004 SPE ATCE held in Houston, Texas, September.
5. Abousleiman, Y., et al.: "Time Effects in Wellbore Fracture Gradient Analysis," presented at the 2005 SPE Applied Technology Workshop "Borehole Strengthening and Stability," The Woodlands, Texas, 18-19 April.
6. Abousleiman, Y. and Nguyen, V.: "Time-Dependent Drilling Fluid Effects on Fracture Gradient Estimation and Possible Misconception of Stress Caging," presented at the 2005 SPE Applied Technology Workshop, Portugal, November.
7. Biot, M. A.: "General Theory of Three Dimensional Consolidation," *J. Appl. Physics*, **12** (1941), 155.
8. Geertsma, J.: "The Effect of Fluid Pressure Decline on Volumetric Changes of Porous Rocks," *Petroleum Trans.*, AIME, **210**(1957a), 331.
9. Geertsma, J.: "A Remark on the Analogy between Thermo elasticity and the Elasticity of Saturated Porous Media," *J. Mech. Phys. Solids*, **6**(1957b), 13.

10. Geertsma, J.: "Problems of Rock Mechanics in Petroleum Production Engineering," Proc. 1st Cong. Int. Soc. Rock Mech., Lisbon, **6** (1966), 585.
11. Morita, N., Black, A. D., and Fuh, G-F.: "Theory of Lost Circulation Pressure," Paper SPE 20409, presented at the 1990 SPE ATCE held in New Orleans, LA, 23-26 September.
12. Fuh, G-F., Morita, N., Boyd, P. A., and McGoffin, S. J.: "A New Approach to Preventing Lost Circulation while Drilling," Paper SPE 24599, presented at the 1992 SPE ATCE held in Washington, DC, 4-7 October.
13. Ito, T., Zoback, M., Peska, p.: "Utilization of Mud Weights in Excess of the Least Principal Stress to Stabilize Wellbores: Theory and Practical Examples," Paper SPE 57007, SPE Drilling and Completion, December, 2001.
14. Fourier, J.B.: *Th´eorie analytique de la chaleur* (*The Analytical Theory of Heat*), Paris (1822).
15. Darcy, H.: *Les fontaines publiques de la Ville de Dijon*, Victor Dalmont, Paris (1856).
16. Hubbert, K. M.: "Darcy's Law and the Field Equations of the Flow of Underground Fluids," *JPT*, **207**(1956), 222.
17. Haimson, B. and Fairhurst, C.: "Initiation and Extension of Hydraulic Fractures in Rocks," *SPEJ*, **7**(1967), 310.
18. Rice, J.R. and Cleary, M.P.: "Some Basic Stress Diffusion Solutions for Fluid Saturated Elastic Porous Media with Compressible Constituents," *J. Appl. Mech.*, **60**(1976), 847.
19. Cui, L., Cheng, A.H.-D., and Abousleiman, Y.: "Poroelastic Solution for an Inclined Borehole," *J. Apple. Mech*. ASME, **64** (1997), 32.
20. Cui, L., Abousleiman, Y., and Cheng, A.H-D.: "Time-dependent Failure Analysis of Inclined Boreholes in Fluid Saturated Formations," *J. Energy Resour. Tech.*, **121**(1997), 31.
21. Abass, H., Shebatalhamd, A., Khan, M., Al-Shobaili, Y., Ansari, A., Ali, S. and Mehta, S.: "Wellbore Instability of Shale Formation; Zuluf Field, Saudi Arabia," Paper SPE SA-609, presented at the 2006 SPE Technical Symposium of Saudi Arabia Section held in Dhahran, Saudi Arabia, May 21-23.
22. Hemphill, T.: "Integrated Management of the Safe Operating Window: Wellbore Stability Is More Than Just Fluid Density," Paper SPE 94732, presented at the 2005 SPE Latin American and Caribbean Petroleum Engineering Conference in Rio de Janeiro, Brazil, June 20-23.
23. Abousleiman, Y., Kanj, M, Ekbote, S,: "Poromechanical Tools for Reservoir Rock Testing Simulation and Wellbore Stability," Paper SPE 71459, presented at the 2001 SPE Annual Technical Conference & Exhibition, New Orleans, Sept.-Oct.
24. Fick, A.: "On Liquids Diffusion," *Philos. Mag.*, **4**, No. 10 (1855), 30.
25. Ekbote, S. and Abousleiman, Y.: "Porochemoelastic Solution for an Inclined Borehole in a Transversely Isotropic Formation," *J. Engng. Mech.*, **132**, No. 7 (2006), 754.
26. Al-Tahini, A.M., Abousleiman, Y.N., and Brumley, J.L.: "Acoustic and Quasistatic Laboratory Measurement and Calibration of the Pore Pressure Prediction Coefficient in the Poroelastic Theory," Paper SPE 95825, presented at the 2005 SPE ATCE, Dallas, TX, Oct. 9-12.

Table 1 - Elastic critical fracturing pressure/mudweight

	S_H	S_h	p_f	KFGLL	Stress Cage	KFGUL
Case A	9200 psi	9000 psi	7000 psi	8900 psi	10000 psi	10800 psi
Case B	6053 psi	5953 psi	3553 psi	12.3 ppg	> 14.4 ppg	17.2 ppg

Table 2 - Time dependency of critical fracturing mudweights for various permeability conditions

	10^{-4} day (8 seconds)	10^{-3} day (1.4 minute)	10^{-1} day (2.4 hours)	1 day
Elastic Permeable	13.62 ppg	13.62 ppg	13.62 ppg	13.62 ppg
Elastic Impermeable	18.90 ppg	18.90 ppg	18.90 ppg	18.90 ppg
Poroelastic $k = 10^2$ mD	16.40 ppg	16.40 ppg	16.40 ppg	16.40 ppg
Poroelastic $k = 10^{-2}$ mD	17.72 ppg	17.28 ppg	16.44 ppg	16.40 ppg
Poroelastic $k = 10^{-5}$ mD	18.01 ppg	18.01 ppg	17.71 ppg	17.28 ppg

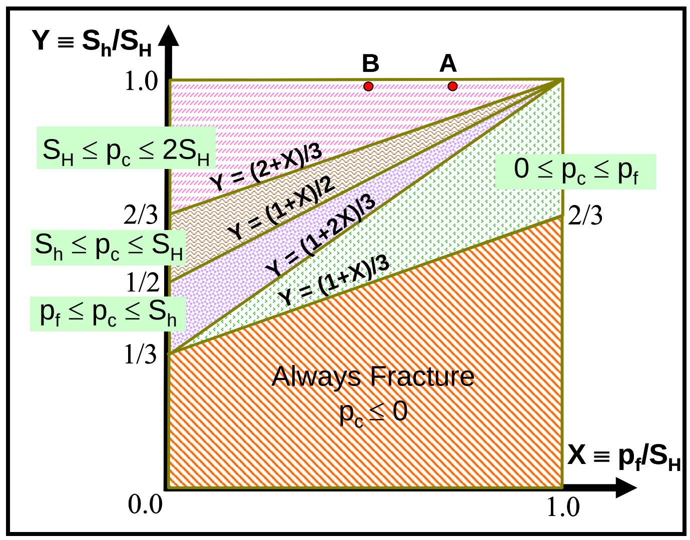

Fig. 1 - Schematic of bounds for fracturing mudweight based on ratios of S_h/S_H and p_f/S_H

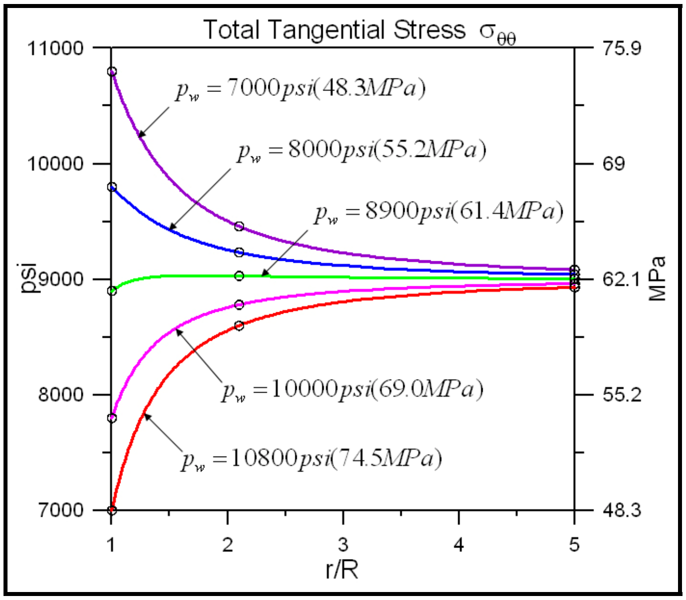

Fig. 2 - Total tangential stress for case A

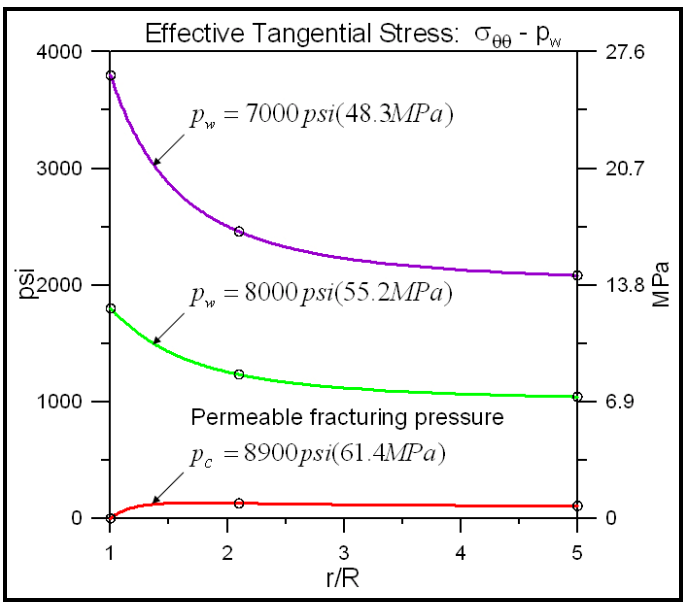

Fig. 3 - Effective tangential stress for permeable borehole wall for case A

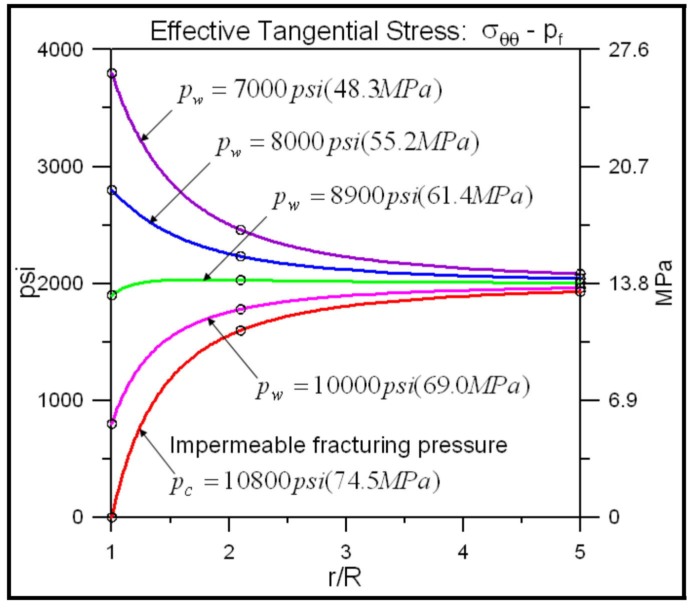

Fig. 4 - Effective tangential stress for impermeable borehole wall for case A

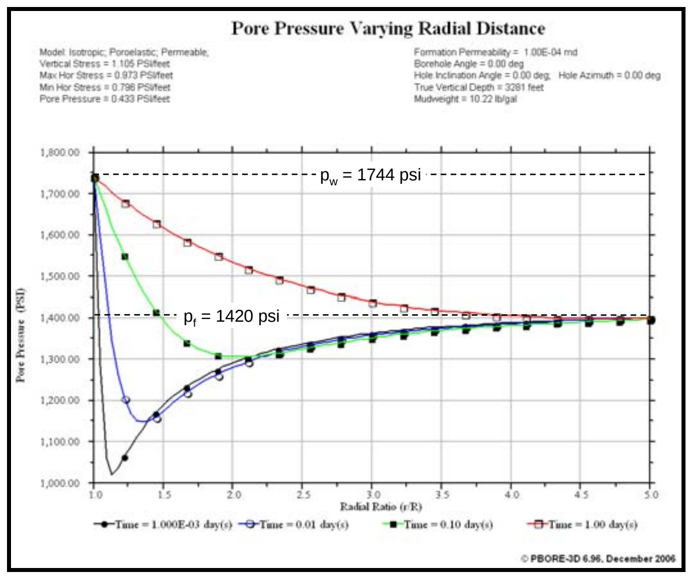

Fig. 5 - Typical pore pressure profile in the formation along the maximum horizontal in-situ stress at various time intervals into drilling

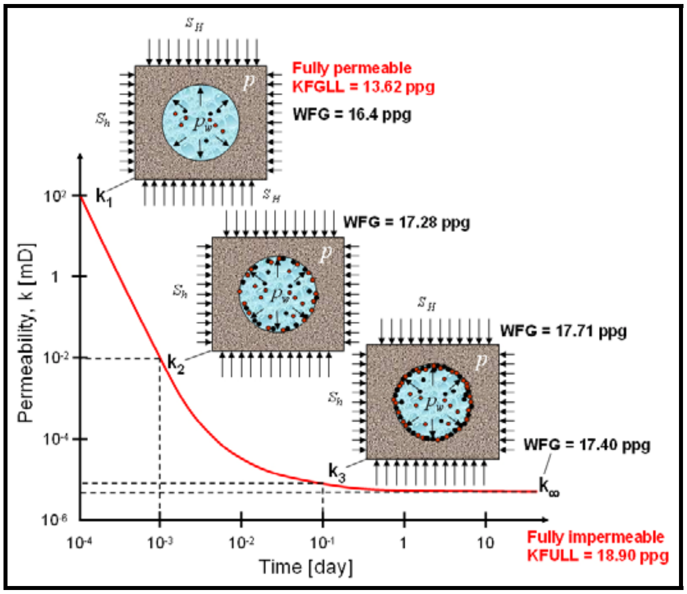

Fig. 6 - Permeability reduction due to LCM/LPM mud circulation in permeable formations

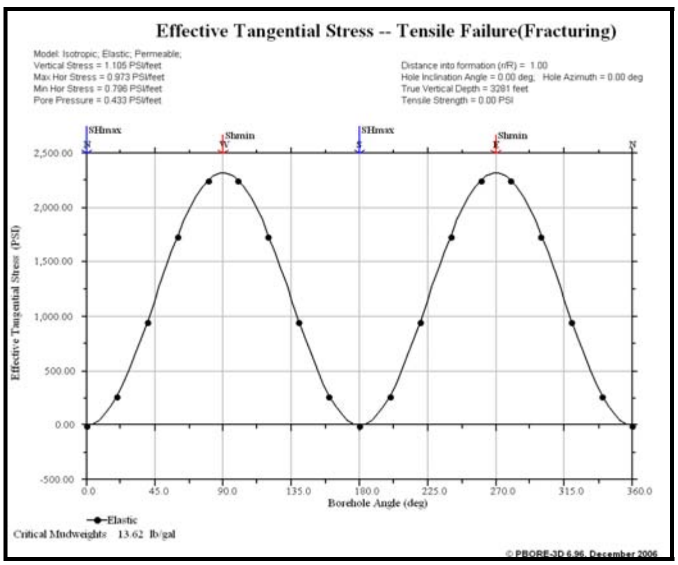

Fig. 7 – Elastic effective tangential stress at and around the borehole wall at critical fracturing mudweight for permeable wall condition

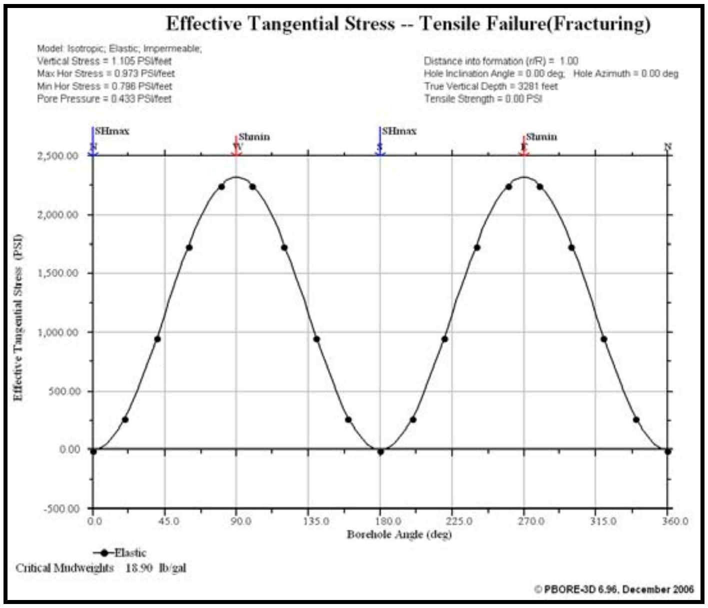

Fig. 8 - Elastic effective tangential stress at and around the borehole wall at critical fracturing mudweight for impermeable wall condition

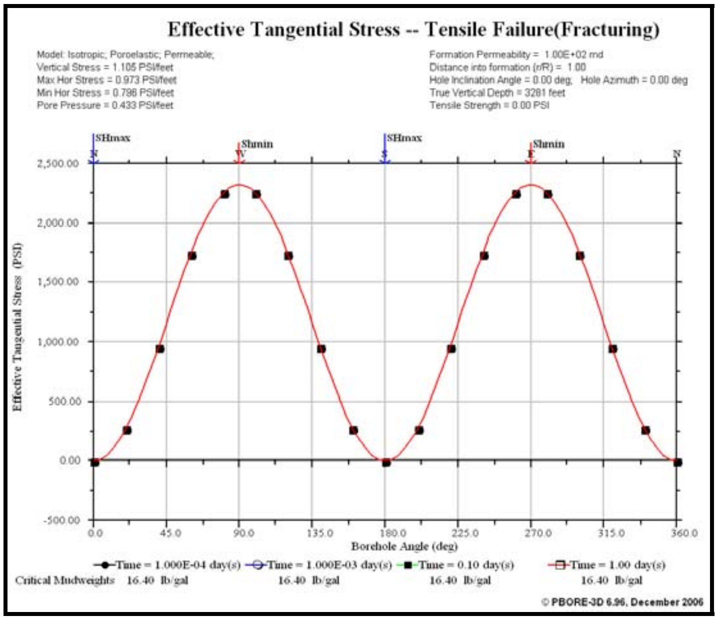

Fig. 9 - Poroelastic effective tangential stress at and around the borehole wall at critical fracturing mudweight for rock formation with near wellbore permeability k = 100 mD at various times into drilling

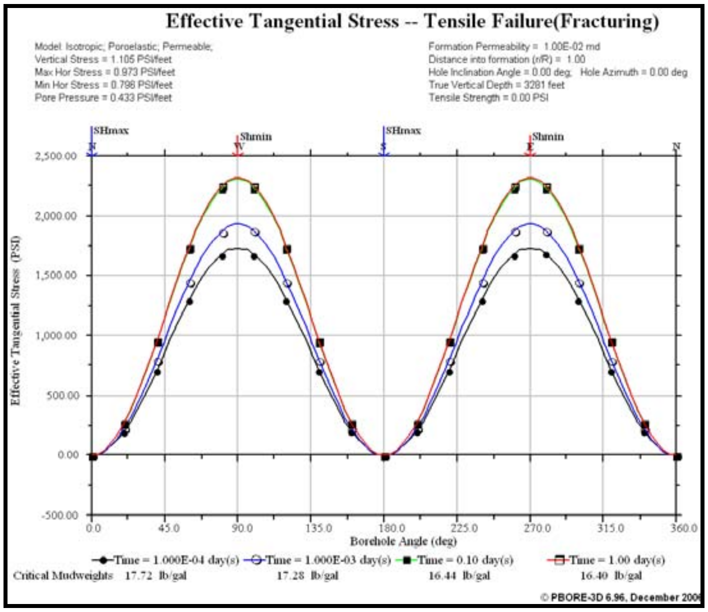

Fig. 10 - Poroelastic effective tangential stress at and around the borehole wall at critical fracturing mudweight for rock formation with near wellbore permeability k = 10^{-2} mD at various times into drilling

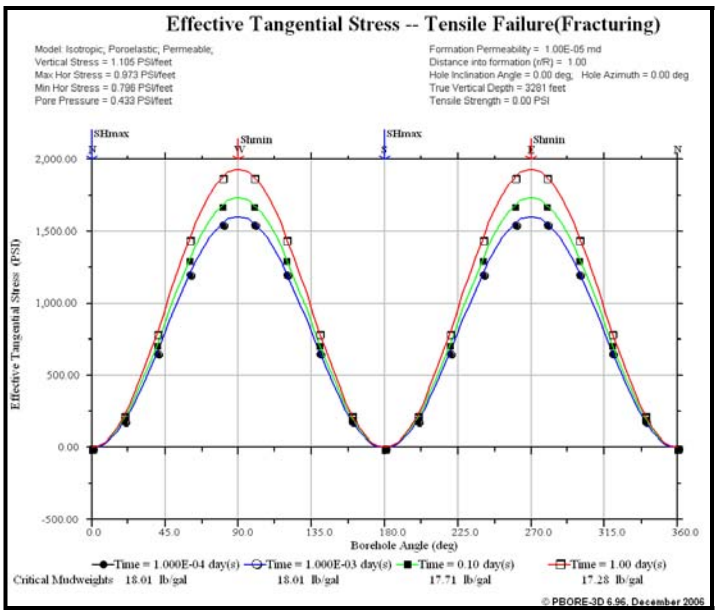

Fig. 11 - Poroelastic effective tangential stress at and around the borehole wall at critical fracturing mudweight for rock formation with near wellbore permeability k = 10^{-5} mD at various times into drilling

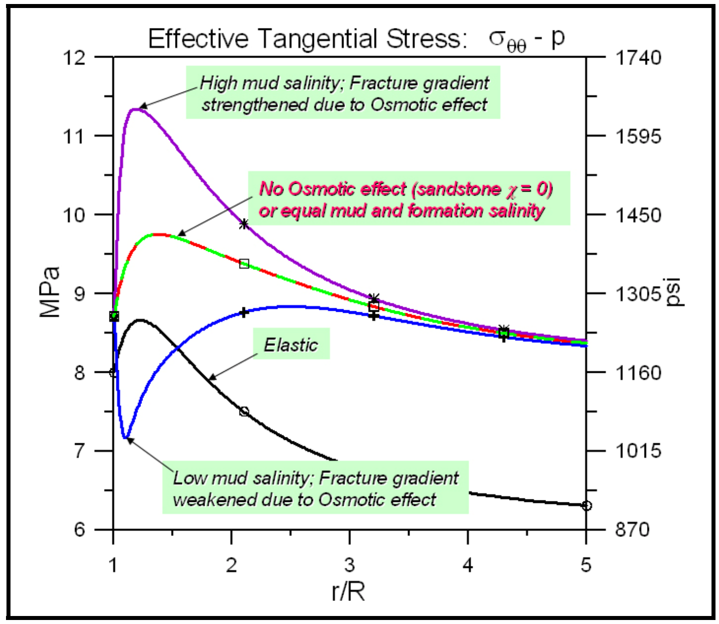

Fig. 12 - Effective tangential stress with and without chemical osmotic effect after 2.4 hours into drilling

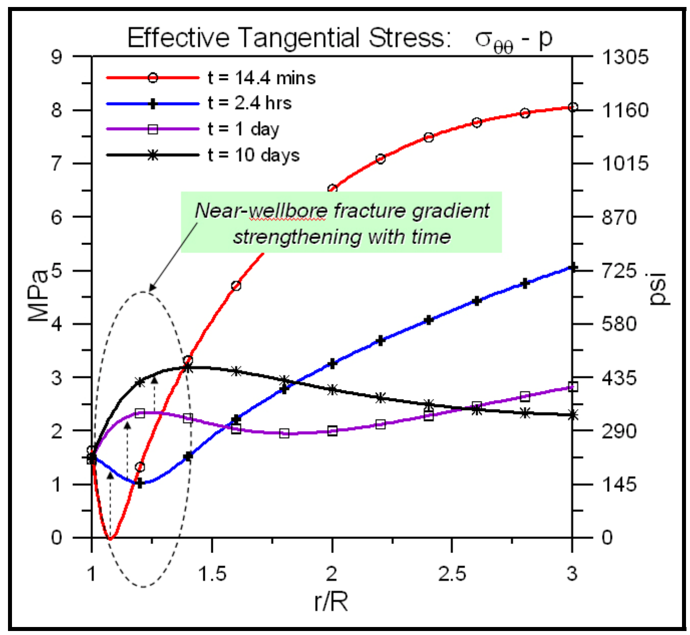

Fig. 13 - Effective tangential stress/fracture gradient strengthening with time due to full porochemoelastic effect